Quality factor affects channel wave propagation in 3D isotropic viscoelastic medium

Hui Li, University of Houston, Peimin Zhu, China University of geosciences, Guangzhong Ji, Xi'an Branch of China Coal Research Institute*

Summary

Due to coal beds existing in the middle of higher velocity wall rocks, seismic wave interferencing with each other generates guide wave propagating within coal beds and surrounding wall rocks (Liu,1994). Three dimensional channel wave propagating within homogeneous isotropic viscoelastic medium containing coal bed is simulated with an explicit, time-domain, high order staggered finite difference algorithm (Carcione, 1998). General standard linear solid (GSLS) system, representing dispersion/attenuation characteristic at both low frequency band and high frequency band, is used to reflect viscoelastic property. Considering massive computational time-consuming, a parallel computational implementation, utilizing OpenMP strategy, allows investigation of large-scale three dimensional models and/or broadband wave propagation within reasonable execution times.

Introduction

Sedimentary rocks and coal beds show viscoelastic characteristic rather than elastic characteristic that generally assumed. Theoretical, numerical, laboratory, and field data indicate that seismic wave through a coal beds is significantly affected by the presence of viscoelastic property. In particular, complicated coupling mechanism of channel wave between wall rocks and coal beds varies with change of quality factors (Q). It is an important physical parameter for attenuation and dispersion of seismic wave. In turn, quality factors (Q) can be used to explain the measurements of channel wave attenuation/dispersion.

In present work, a time-domain high-order staggered grid finite difference (FD) algorithm is developed for numerically solving viscoelastic wave equations in three dimensional spatial dimensions. Our algorithm is an adaptation of the high order staggered grid velocity-stress approach.

Theory and Method

According to viscoelastic theory (Mou, 2003), stress (σ_{ij}) and strain (δ_{ij}) relations can be expressed as follows

$$\sigma_{ij} = \dot{\Lambda} * \delta_{ij}\varepsilon_{kk} + 2\dot{M} * \delta_{ij} \tag{1}$$

Stress and velocity (v_j) relations can be given:

$$\dot{\varepsilon}_{ij} = \frac{1}{2}(\partial_i \upsilon_j + \partial_j \upsilon_i) \tag{2}$$

Assuming $\Pi = \Lambda + 2M$, then we known for GSLS model

$$\Pi = \pi[1 - \sum_{l=1}^{L}(1 - \frac{\tau_{\varepsilon l}^{p}}{\tau_{\sigma l}})e^{-t/\tau_{\sigma l}}]\theta(t) \tag{3}$$

$$M = \mu[1 - \sum_{l=1}^{L}(1 - \frac{\tau_{\varepsilon l}^{s}}{\tau_{\sigma l}})e^{-t/\tau_{\sigma l}}]\theta(t) \tag{4}$$

respectively. In the formulation, $\pi = \lambda + 2\mu$, λ, μ indicates lame elastic coefficients. $\theta(t)$ denotes memory variable. Π, M depend on relaxation constant of P-wave strain ($\tau_{\varepsilon l}^{p}$) and S-wave strain ($\tau_{\varepsilon l}^{s}$), respectively. Then substituting equation (3), (4) into (1).

$$\dot{\sigma}_{ij} = (\dot{\Pi} - 2\dot{M}) * \partial_k \upsilon_k + 2\dot{M} * \partial_i \upsilon_j, \quad i = j \tag{5a}$$

$$\dot{\sigma}_{ij} = \dot{M} * (\partial_i \upsilon_j + \partial_j \upsilon_i), \quad i \neq j \tag{5b}$$

Then substituting equations (3) and (4) into (5a) and (5b), stress equation can be given by linear approximation

$$\dot{\sigma}_{ij} = \{\pi[1 - \sum_{l=1}^{L}(1 - \frac{\tau_{\varepsilon l}^{p}}{\tau_{\sigma l}})] - 2\mu[1 - \sum_{l=1}^{L}(1 - \frac{\tau_{\varepsilon l}^{s}}{\tau_{\sigma l}})]\} \partial_k \upsilon_k + 2\mu[1 - \sum_{l=1}^{L}(1 - \frac{\tau_{\varepsilon l}^{s}}{\tau_{\sigma l}})]\partial_i \upsilon_j + \sum_{l=1}^{L} r_{ijl}, \quad i = j \tag{6a}$$

$$\dot{\sigma}_{ij} = \mu[1 - \sum_{l=1}^{L}(1 - \frac{\tau_{\varepsilon l}^{s}}{\tau_{\sigma l}})](\partial_i \upsilon_j + +\partial_j \upsilon_i) + \sum_{l=1}^{L} r_{ijl}, \quad i \neq j \tag{6b}$$

And memory variable equations can be given

$$\dot{r}_{ijl} = -\frac{1}{\tau_{\sigma l}}\{r_{ijl} + [\pi(\frac{\tau_{\varepsilon l}^{p}}{\tau_{\sigma l}} - 1) - 2\mu(\frac{\tau_{\varepsilon l}^{s}}{\tau_{\sigma l}} - 1)]\partial_k \upsilon_k + 2\mu(\frac{\tau_{\varepsilon l}^{s}}{\tau_{\sigma l}} - 1)]\partial_i \upsilon_j\}$$

DOI http://dx.doi.org/10.1190/segam2012-1180.1

$$1 \le l \le L, i = j \tag{7a}$$

$$\dot{r}_{ijl} = -\frac{1}{\tau_{\sigma l}}[r_{ijl} + \mu(\frac{\tau_{\varepsilon l}^{s}}{\tau_{\sigma l}} - 1)(\partial_i \upsilon_j + \partial_j \upsilon_i)],$$

$$1 \le l \le L, i \ne j \tag{7b}$$

For particle velocity equation is given

$$\rho \dot{\upsilon}_i = \partial_j \sigma_{ij} + f_i \tag{8}$$

f_i denotes external force, $i, j, k = x, y, z$. π is function of P-wave velocity, P-wave relaxation time, and frequency; μ is function of S-wave velocity, S-wave relaxation time, and frequency.

The relations between relaxation time and P-wave quality factor (Q_P) and S wave quality factor (Q_s) are given

$$\tau_{\sigma} = \frac{1}{\omega}(\sqrt{1 + \frac{1}{Q_P^2}} - \frac{1}{Q_P}), l = 1 \tag{9a}$$

$$\tau_{\varepsilon}^{p} = \frac{1}{\omega^2 \tau_{\sigma}}, \tau_{\varepsilon}^{s} = \frac{1 + \omega_0 \tau_{\sigma} Q_s}{\omega Q_s - \omega^2 \tau_{\sigma}} \tag{9b}$$

respectively. ω denotes domain frequency. When $L = 1$, the above equations can be deteriorated into standard linear viscoleastic equations.

O(2,N) Staggered Grid Finite Difference Scheme

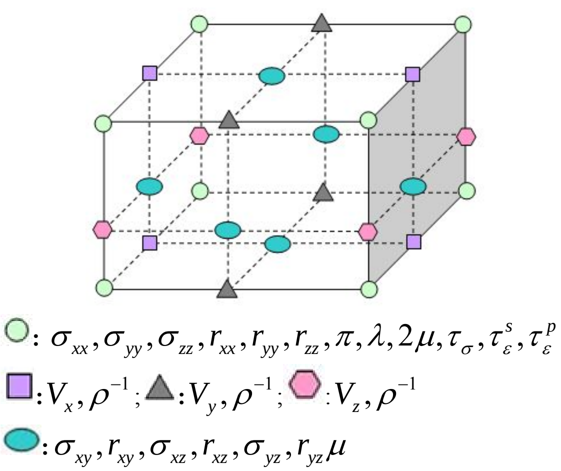

Figure 1: Staggered spatial storage scheme for the 22 viscoelastic dependent variables

The partial differential equations (6a), (6b), (7a), (7b) and (8) are numerically solved with an explicit, time-domain high order staggered grid finite difference technique. Dependent variables are stored on staggered spatial and temporal grids. Figure 1 depicts the distribution of the dependent variables over an elementary cell of the 3D grid. All spatial derivatives are approximated with high order staggered FD operators processing N[th] order (4[th] order is used in this paper) accuracy in the discretization intervals. Stresses are stored on the integer time raster tn, and velocities are stored on the interlaced half-integer time raster tn+Δt/2, where Δt is time step. Temporal FD operators are centered and have 2[nd] order accuracy.

These FD updating formulates are (only showing one component)

$$\begin{aligned}
&\sigma_{xx}^{n+}(i,j,k) = \sigma_{xx}^{n-}(i,j,k) + \pi(i,j,k)\Delta t \\
&\{[1 + \sum \tau^{P}(i,j,k)]\{L_x^-[v_x^n(i^+,j,k)] \\
&+ L_y^-[v_y^n(i,j^+,k)] + L_z^-[v_z^n(i,j,k^+)]\}\} \\
&-2\mu(i,j,k)\Delta t[1 + \sum \tau^{s}(i,j,k)] \\
&\{L_y^-[v_y^n(i,j^+,k)] + L_z^-[v_z^n(i,j,k^+)]\} \\
&+ \frac{\Delta t}{2}\sum_{l=1}^{L}[R_{xxl}^{n+}(i,j,k) + R_{xxl}^{n-}(i,j,k)]
\end{aligned} \tag{10}$$

$$\begin{aligned}
&\sigma_{xz}^{n+}(i,j,k) = \sigma_{xz}^{n-}(i,j,k) + \mu(i,j,k)\Delta t \\
&[1 + \sum \tau^{s}(i,j,k)]\{L_x^-[v_z^n(i,j,k^+)] \\
&+ L_z^-[v_x^n(i^+,j,k)]\} + \frac{\Delta t}{2} \\
&\sum_{l=1}^{L}[R_{xzl}^{n+}(i,j,k) + R_{xzl}^{n-}(i,j,k)]
\end{aligned} \tag{11}$$

$$\begin{aligned}
&R_{xxl}^{n+}(i,j,k) = (1 + \frac{\Delta t}{2\tau_{\sigma l}})^{-1}\{(1 - \frac{\Delta t}{2\tau_{\sigma l}})R_{xxl}^{n-}(i,j,k) \\
&-\frac{\pi(i,j,k)}{\tau_{\sigma l}}\tau^{P}(i,j,k)\{L_x^-[v_x^n(i^+,j,k)] \\
&+ L_y^-[v_y^n(i,j^+,k)] + L_z^-[v_z^n(i,j,k^+)]\}
\end{aligned}$$

 DOI http://dx.doi.org/10.1190/segam2012-1180.1

$$\frac{2\mu(i,j,k)\Delta t}{\tau_{\sigma l}}\tau^{s}(i,j,k)$$
$$\{L_y^-[v_y^n(i,j^+,k)]+L_z^-[v_z^n(i,j,k^+)]\}\} \quad (12)$$

$$R_{xzl}^{n+}(i,j,k)=(1+\frac{\Delta t}{2\tau_{\sigma l}})^{-1}\{(1-\frac{\Delta t}{2\tau_{\sigma l}})R_{xzl}^{n-}(i,j,k)$$
$$-\frac{\mu(i,j,k)\Delta t}{\tau_{\sigma l}}\tau^{s}(i,j,k)\{L_x^-[v_z^n(i,j,k^+)]$$
$$+L_z^-[v_x^n(i^+,j,k)]\} \quad (13)$$

$$v_x^{n+}(i^+,j,k)=v_x^{n-1}(i^+,j,k)+\frac{\Delta t}{\rho(i^+,j,k)})$$
$$\{L_x^+[\sigma_{xx}^{n-}(i,j,k)]+L_y^-[\sigma_{xy}^{n-}(i^+,j^+,k)] \quad (14)$$
$$+L_z^-[\sigma_{xz}^{n-}(i^+,j,k^+)]+f_x^n(i^+,j,k)\}$$

For the above formulates, Δt denotes time interval, superscript n+ and n- denote n+1/2 and n-1/2, respectively. L is differential operators given

$$L_x^+[u(x)]=\frac{1}{\Delta x}\sum_{i=1}^{N}C_i^{(N)}\{u(x+i\Delta x)-u[x-(i-1)\Delta x]\}$$
$$L_x^-[u(x)]=\frac{1}{\Delta x}\sum_{i=1}^{N}C_i^{(N)}\{u[x+(i-1)\Delta x]-u(x-i\Delta x)\} \quad (15)$$

Synthetic Data Example

Timeslices in figures 2 illustrate 3D viscoelastic channel wave propagation in the model (200m*200m*100m) consisting of coal beds (thickness is 10m, from z=45m to z=55m). A point explosion source activated by a Ricker wavelet (domain frequency 120Hz) is located at coal beds (5m,100m,50m).

Fine spatial (x=y=1m, z=0.5m) and temporal (0.1ms) gridding are required for representation of channel wave, without numerical dispersion. A parallel algorithm implementation, utilizing OpenMP strategy, allows this large model to be investigated in reasonable execution time.

Physical parameters and quality factors distribution are displayed in Table 1 and Table 2, respectively. In the table 2, Qp_w and Qs_w denote p-wave quality factor of wall rock and s-wave quality factor of wall rock, respectively. Qp_c and Qs_c denote p-wave quality factor of coal and s-wave quality factor of coal, respectively.

Table 1: strata physical parameters

P-wave m/s	S-wave m/s	Density (g/cm3)	thick m	lithology
2800	1618	2.2	95	Sandstone
2200	1270	1.4	10	Coal bed
2800	1618	2.2	95	Sandstone

Table 2: Quality factor distribution

Model	Qp_w	Qs_w	Qp_c	Qs_c
1	25	15	10	5
2	40	20	20	9
3	80	40	50	22
4	140	75	100	45

Discussion of results/Conclusion

Figure 2 shows Vx component (left column) and Vz component (right column) snapshot in the 45ms.

For the Vx component, channel wave, concentrating mostly seismic wave energy, propagates in the coal bed. Only a little energy still leaks into wall rock. Less energy transmission happens as the quality factors (both wall rock and coal beds) increase. But intensity of shear wave of wall rock slightly increases when quality factors increasing. For the channel wave, the energy seems remain stable as quality factors increase.

For the Vz component, although channel wave concentrates mostly seismic wave energy, partly energy transmitting into wall rock propagates as shear wave velocity of wall rock. As quality factors increase, the intensity of compressional wave of wall rock decreases dramatically, but for shear wave of wall rock, it still keeps almost constant.

Considering of contrast of intensity of wall rock and coal beds, the Vx component has higher channel wave transmission wave ratio, and the ratio keeps relatively stable while quality factors increase/decrease. In turn, Vx component may be more advantage for channel wave exploration.

DOI http://dx.doi.org/10.1190/segam2012-1180.1

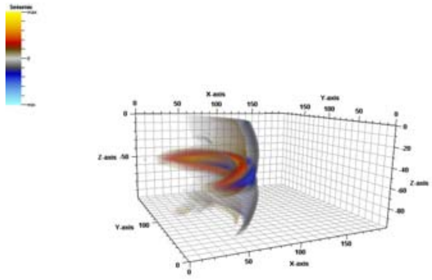

Model 1 Vx 45ms

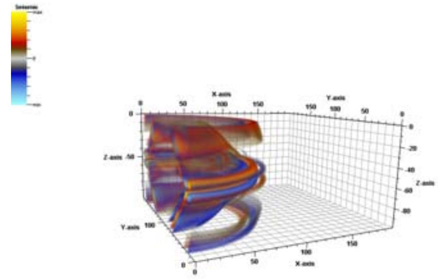

Mode1 Vz 45ms

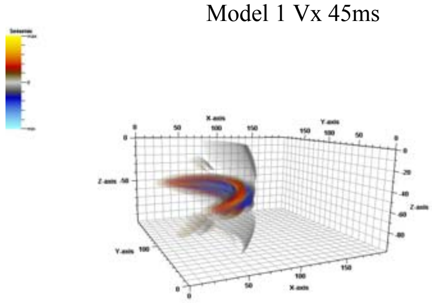

Model 2 Vx45ms

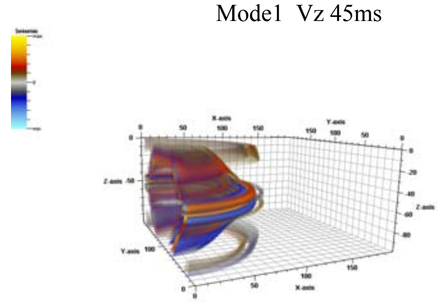

Mode 2 Vz 45ms

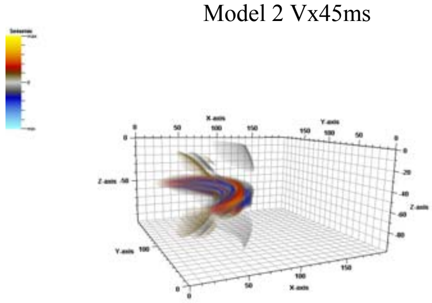

Model 3 Vx 45ms

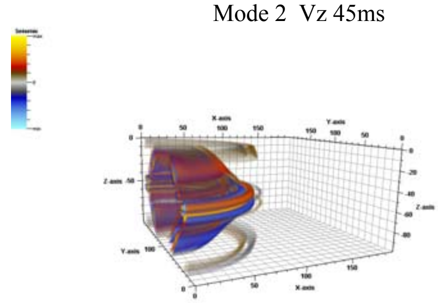

Mode 3 Vz 45ms

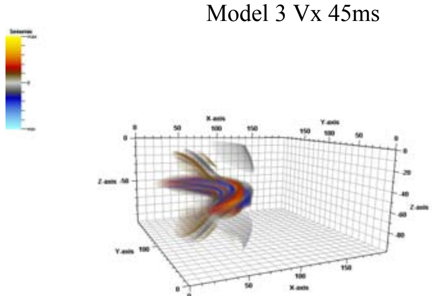

Model 4 Vx 45ms

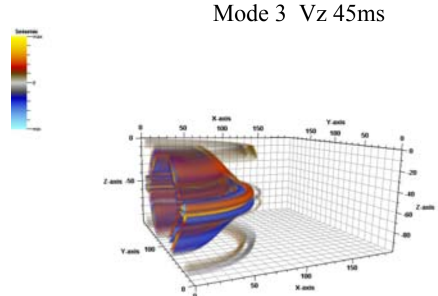

Mode 4 Vz 45ms

Figure 2: Vx and Vy component snapshot at 45ms

http://dx.doi.org/10.1190/segam2012-1180.1

EDITED REFERENCES

Note: This reference list is a copy-edited version of the reference list submitted by the author. Reference lists for the 2012 SEG Technical Program Expanded Abstracts have been copy edited so that references provided with the online metadata for each paper will achieve a high degree of linking to cited sources that appear on the Web.

REFERENCES

Carcione, J., 1998, Visco-acoustic wave propagation simulation in the earth: Geophysics, **53**, 769–777.

Liu, T. F., D. M. Pan, 1994, In-seam seismic exploration: China University of Mining and Technology Press.

Mou, Y. G., 2005, Seismic numerical modeling for 3D complex media: Petroleum Industry Press.